References

1. (a) Menger, F. M.; Whitesell, L. G. *J. Am. Chem. Soc.* **1985**, *107*, 707. (b) Moss, R. A.; Kim, K. Y.; Swarup, S. *ibid.* **1986**, *108*, 788. (c) Menger, F. M.; Gan, L. H.; Johnson, E.; Durst, D. H. *ibid.* **1987**, *109*, 2800. (d) Mackay, R. A.; Longo, F. R.; Knier B. L.; Durst, H. D. *J. Phys. Chem.* **1987**, *91*, 861. (e) Moss, R. A.; Ganguli, S. *Tetrahedron Lett.* **1989**, *30*, 2071. (f) Lee, Y. H.; Park, H.; Choi, K. N.; Chang, S. I.; Kim, T. H. *J. of Korean Ind. & Eng. Chemistry* **1994**, *5*, 114.
2. Park, B. D.; Lee, Y. S. *Bull. Korean. Chem. Soc.* **1992**, *13*(1), 5.
3. Park, B. D.; Lee, Y. S. *ibid.* **1992**, *13*(4), 357.
4. Bucherer, H. T.; Lieb, V. A. *J. Prakt. Chem.* **1934**, *141*(2), 5.
5. Frost, A. A.; Pearson, R. G. Kinetics and Mechanism; 2nd ed., Wiley: New York, 1961, pp 166-169.
6. Smith, M. A.; Applegate, V. C.; Johnson, B. G. H. *J. Chem. Eng. Data* **1961**, *6*, 607.
7. Rook, J. J. *Environ. Sci. & Technol.* **1977**, *11*, 478.
8. Soulard, M.; Block, F.; Hatterrer, A. *J. Chem. Soc. Dalton Trans.* **1981**, 2300.
9. Kumar, K.; Margerum, D. W. *Inorg. Chem.* **1987**, *26*, 2706.
10. (a) Mills, J. F.; Schneider, J. A. *Ind. End. Chem. Prod. Res. Dev.* **1973**, *12*, 160. (b) Jolly, R. L. Water Chlorination Environmental Impact and Health Effects; Ann Arbor Sci. **1975**, pp 21-77. (c) Voudrias, E. A.; Reinhard, M. *Environ. Sci. & Technol.* **1988**, *22*, 1049.
11. Minato, H.; Takeda, K.; Miura, T.; Kobayashi, M. *Chem. Letter* **1977**, 1095.
12. Kurz, J. L. *J. Phys. Chem.* **1962**, *66*, 2239.

Crystal Geometry Optimization of β-Lactam Antibiotics Using MMFF Parameters

Youngdo Won

Department of Chemistry, Hanyang University, Seoul 133-792, Korea

Received June 26, 1995

A generic force field approach has been applied to geometry optimization of penam and cephem crystals. The crystalline state energy and force evaluation with the universal force field (MMFF : Merck Molecular Force Field) results in good agreements with the crystallographic data. Bond lengths are usually correct to within 0.02 Å and bond angles usually to within 2.5° The conformation of the β-lactam bicyclic rings in the crystal environment is also well reproduced. The results thus demonstrate the applicability of MMFF to modeling of newer molecular constructs in condensed phase.

Introduction

Since the molecular mechanics (MM2) force field was first introduced by Allinger in the late 1970s,[1] there have been concentrated efforts in optimizing transportable force fields suitable for simulations of liquid states and complex macromolecular assemblies. Among the most widely used are the MM2[1,2] and MM3[3] force fields useful for studying a variety of organic and inorganic systems and the AMBER (Assisted Model Building with Energy Refinement) force fields[4] of Kollman and co-workers and the CHARMM (Chemistry at HARvard Macromolecular Mechanics) force fields[5] of Karplus and co-workers for proteins and nucleic acids.

Despite these efforts, one often encounters the problem of "missing parameters" in a routine computational chemistry application dealing with new molecular moieties. The molecular construct could be a newly designed receptor or a potent therapeutic agent. Because it is not clear how to generalize force field parameters for similar atoms in slightly different environments, one has to develop a suitable parameter set for the new molecule and thoroughly check its validity in one's intended research, which is a time consuming and challenging procedure.

In order to facilitate molecular modeling research of molecular systems with little or no experimental data available (and as a consequence, with no readily available force field parameters), a few generic force fields have been considered: DREIDING of Goddard and co-workers,[6] UFF (Universal Force Field) of Rapp and co-workers,[7] VALBOND of Landis and co-workers[8] and MMFF (Merck Molecular Force Field) of Halgren and co-workers.[9] The generic force fields have certain advantages in dealing with new molecular constructs that have never been parameterized, because they can theoretically cover the entire periodic table. Inorganic systems including transition metals as well as macromolecular systems with the molecular structure far from equilibrium can be easily modeled with the generic force fields.

In this work, we have optimized several penam and cephem crystals using the most recent MMFF parameter set. Penicillins and cephalosporins are β-lactam antibiotics that inhibit the transpeptidases and carboxypeptidases involved in the biosynthesis of the peptidoglycan bacterial cell walls.[10] The biological activity of these compounds is strongly related to the reactivity of the β-lactam ring.[11] For the ratio-

nal design of a potent ligand useful for pharmaceutical applications, we need to understand the energetics and conformations of the β-lactam ring fused with the 5- or 6- membered ring system.

Theoretical calculations on the penam and cephem derivatives have been challenging research problems. The sulphur atom in the 5- or 6-membered ring makes *ab initio* calculations with an extended basis set (even at the 6-31G level) computationally demanding. The β-lactam nitrogen atom assumes an irregular geometry not pyramidal nor planar, which makes the normal parameter set with sp^2 or sp^3 nitrogen atoms unsuitable for molecular mechanical calculations. The crystal calculations thus provide a series of tests for usefulness of the newly developed generic force field and also lay out the ground for further developments of the parameter set useful for β-lactam antibiotics design.

Theory

MMFF has been derived from a large number of high level *ab initio* calculations. In order to be widely applicable, it could not be parameterized against particular experimental data. There are few high quality experimental data available, especially for conformational and intermolecular interaction energies. However, MMFF employs effective pair potentials which reflect the charge distribution in a high dielectric medium due to molecular polarizability. Therefore, MMFF is readily applicable to condensed phase simulations. The detailed procedure for MMFF parameterization against objectively defined quantum mechanical data is described elsewhere by the original developers.[9] Here, we specify only the functional form and the current version of the parameter set used in this work.

The MMFF energy is partitioned into individual energy terms similar to the standard molecular mechanical potential function.

$$E=\sum E_{B_{ij}}+\sum E_{A_{ijk}}+\sum E_{BA_{ijk}}+\sum E_{OOP_{ijk;l}}+\sum E_{T_{ijkl}}+\sum E_{vdW_{ij}}+\sum E_{Q_{ij}} \quad (1)$$

Bond Stretching. The quartic function is employed for bond stretching terms,

$$E_{B_{ij}}=\frac{143.9325}{2}k_{b_{ij}}\Delta^2_{r_{ij}}\left[1+C_s\Delta_{r_{ij}}+\frac{7}{12}C_s^2\Delta^2_{r_{ij}}\right] \quad (2)$$

where $k_{b_{ij}}$ is the force constant, $\Delta_{r_{ij}}=r_{ij}-r_{ij}^o$ is the difference between actual and reference bond lengths, and $C_s=-2$ Å^{-1} is the "cubic stretch" constant. The function corresponds to an expansion through the fourth order of a Morse function.

Angle Bending. The cubic polynomial form is normally used.

$$E_{A_{ijk}}=\frac{0.043844}{2}k_{a_{ijk}}\Delta^2_{T_{ijk}}[1+C_b\Delta_{T_{ijk}}] \quad (3)$$

where $k_{a_{ijk}}$ is the force constant, $\Delta_{T_{ijk}}=\theta_{ijk}-\theta^o_{ijk}$ is the difference between actual and reference bond angles, and $C_b=-0.007$/deg is the "cubic-bend" constant. For linear or near-linear bond angles, the well-behaved form used in DREIDING[6] and UFF[7] is employed.

$$E_{A_{ijk}}=\frac{0.043844}{2}k_{a_{ijk}}[1+\cos\theta_{ijk}] \quad (4)$$

Stretch-Bend Interactions. The following form is used for 1-3 interactions.

$$E_{BA_{ijk}}=2.51210(k_{ba_{ijk}}\Delta_{r_{ij}}+k_{ba_{kji}}\Delta_{r_{kj}})\Delta_{T_{ijk}} \quad (5)$$

where $k_{ba_{ijk}}$ and $k_{ba_{kji}}$ are force constants which couple the i-j and k-j bond stretches to the i-j-k bend. Stretch-bend interactions are not used for linear bond angles.

Out-of-Plane Bending. The out-of-plane bending at a tricoordinate center is described by

$$E_{OOP_{ijk;l}}=\frac{0.043844}{2}k_{OOP_{ijk;l}}\omega^2_{ijk;l} \quad (6)$$

where $k_{OOP_{ijk;l}}$ is the force constant and $\omega_{ijk;l}$ is the angle between the bond j-l and the plane i-j-k.

Torsion Interactions. The three-fold representation of MM2 and MM3 is used for dihedral interactions.[1-3]

$$E_{T_{ijkl}}=\frac{1}{2}[V_1(1+\cos\phi)+V_2(1-\cos2\phi)+V_3(1+\cos3\phi)] \quad (7)$$

Van der Waals Interactions. MMFF employs the recently developed "Buffered 14-7" form.[12]

$$E_{vdW_{ij}}=\varepsilon_{ij}\left(\frac{1.07R_{ij}^*}{R_{ij}+0.07R_{ij}^*}\right)^7\left(\frac{1.12R_{ij}^{*7}}{R_{ij}^7+0.12R_{ij}^{*7}}-2\right) \quad (8)$$

A specially formulated combination rule for the minimum-energy separation R_{ij}^* and a Slater-Kirkwood expression for the well depth ε_{ij} are detailed in Ref. 12.

Electrostatic Interactions. For electrostatic interaction energy terms, the buffered Coulombic form is employed.

$$E_{Q_{ij}}=332.0716\frac{q_iq_j}{\varepsilon(R_{ij}+\delta)} \quad (9)$$

where q_i and q_j are partial atomic charges, R_{ij} is the internuclear separation, $\delta=0.05$ Å is the "electrostatic buffering" constant, and is the dielectric constant. Partial atomic charges, q_i, are constructed from formal atomic charges, q_i^o, by adding contributions from bond charge increments q_{ki} which describe the polarity of the bonds to atom i from attached atoms k.

$$q_i=q_i^o+\sum_k q_{ki} \quad (10)$$

where $q_{ik}=-q_{ki}$. Normally, the dielectric constant is set to one and 1,4-interactions are scaled by a factor of 0.75.

The refinement/improvement of the MMFF parameter set is an on-going development project. The current parameter files used in this work are listed in Table 1. The last revision date is indicated in the table, otherwise the file is as current as the latest revision date.

Computational Procedure

The force field described in the previous section has been incorporated in a developmental version of CHARMM (c24x 1) and a commercial version of CHARMm (22r3) of Molecular Simulations Inc. It is thus possible to use most CHARMM functions with MMFF. In this work, we used QUANTA 4.0

Table 1. The MMFF Parameter Files

File	Contents	Last Revision
MMFFDEF.PAR	Primary definitions	
MMFFHDEF.PAR	Symbolic types for hydrogen	
MMFFSYMB.PAR	Symbol type definitions	
MMFFPROP.PAR	Atom type properties	
MMFFAROM.PAR	Aromatic symbol types	
MMFFBOND.PAR	Bond parameters	29-Oct-93
MMFFBNDK.PAR	Bond default rule parameters	
MMFFANG.PAR	Angle parameters	5-Nov-93
MMFFSTBN.PAR	Stretch-bend parameters	
MMFFDFSB.PAR	Default stretch-bend parameters	
MMFFOOP.PAR	Out-of-plane parameters	
MMFFTOR.PAR	Torsion parameters	15-Oct-93
MMFFCHG.PAR	Bond-charge increments	10-Nov-93
MMFFPBCI.PAR	Partial bond-charge increments	14-Oct-93
MMFFVDW.PAR	van der Waals parameters	28-Sep-93

and CHARMm22r3 available on a SGI platform running under the IRIX 4.0.5 operating system.

We searched the Cambridge Structural Database (CSD) and obtained crystal structures suitable for crystal simulations using CHARMm22r3 (the CHARMM/MMFF version). In order to evaluate energies and forces with MMFF in CHARMM, atomic connectivity must be specified with the bond order, which is not supported in the normal CHARMM RTF (Residue Topology File) data structure. Several QUANTA functions are used to convert CSD files into the Merck molecular data format. First, we read a CSD file and put proper bond order information onto the molecular structure by using the molecular editor function. Then, the QUANTA command "data write Merck" is used to generate the molecular data file needed for MMFF energy/force evaluation. In order to scale 1-4 interactions as specified in MMFF, we set the E14FAC value of CHARMM to 0.75. The default is 0.5 in the normal CHARMM version.

With the molecular structure input in the Merck format, the CHARMM CRYStal facility is used to build the crystal structure. The crystal build cutoff distance is set to 15.0 Å, the same as the CUTNB distance used for nonbond pair list generation. For the shifted smoothing function applied to non-bonded energy evaluation, the CTOFNB cutoff distance is used to generate the shifted potential and the switching function uses both CTONNB and CTOFNB to switch on and off the potential smoothing function. The nonbond CTONNB and CTOFNB distances are set to 10.0 and 12.0 Å, respectively. The distance scaled dielectric constant (RDIE) option is employed for electrostatic interactions, which reproduces crystal lattice constants better than the CDIE (constant dielectric) option. ATOM/SHIFT/VATOM/

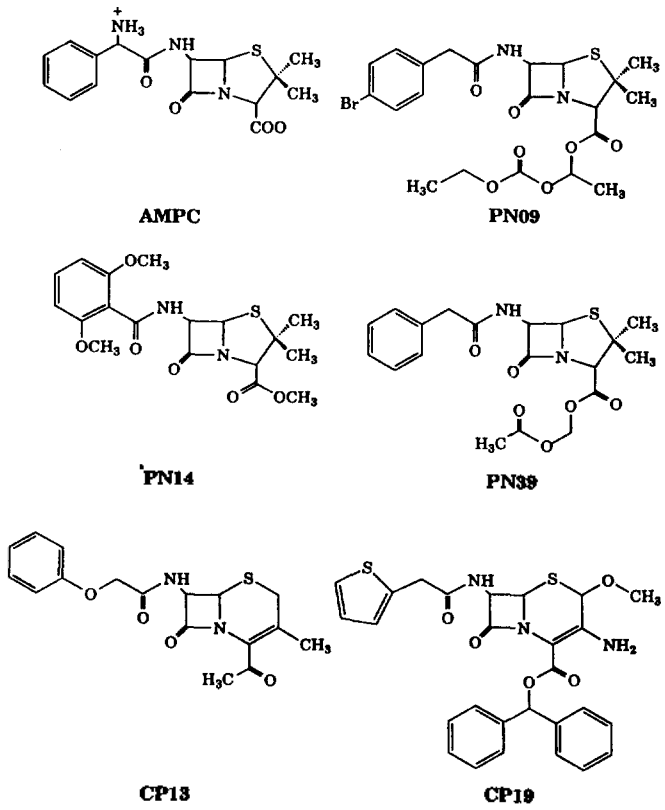

Figure 1. Unit Cell molecular structure formulae. The crystal structures are obtained from CSD (Cambridge Structural Database). The full compound name is abbreviated by the four character code as follows: AMPC = 6-(D-(−)-α-Aminophenyl-acetoamido)-penicillanic acid, PN09 = p-Bromobenzyl-penicillin 1'-diethylcarbonate ester, PN14 = (2,6-Dimethoxyphenyl)-penicillin methyl ester, PN39 = Penicillin-G-acetoxymethylester, CP13 = 4-Acetyl-3-methyl-7-β-phenoxyacetamido-Δ^3-cephem, and CP19 = 3-Amino-4-methoxy-cephalothin benzhydryl ester.

Table 2. Penam and Cephem Crystal Data from CCDB[a]

	Crystal System	Unit Cell Volume	a	b	c	α	β	γ	Space Group
AMPC	monoclinic	839.5	12.400	6.200	12.000	90.0	114.50	90.0	$P2_1$
PN09	orthorhombic	2404.0	21.555	12.994	8.583	90.0	90.0	90.0	$P2_12_12_1$
PN14	monoclinic	964.5	14.728	9.733	6.901	90.0	102.85	90.0	$P2_1$
PN39	monoclinic	1020.6	12.912	8.087	10.137	90.0	105.38	90.0	$P2_1$
CP13	orthorhombic	1667.8	23.771	8.833	7.943	90.0	90.0	90.0	$P2_12_12_1$
CP19	orthorhombic	2655.0	10.912	8.691	27.996	90.0	90.0	90.0	$P2_12_12_1$

[a] lengths are given in Å and angles are in degrees.

Table 3. Optimized Crystal Constants[a]

	Initial Gradient Norm[b]	Unit Cell Volume	a	b	c	α	β	γ	RMS dev.
AMPC	16.272	812.3	12.120	6.093	12.040	90.0	114.0	90.0	1.162
PN09	0.867	2532.5	21.815	13.402	8.662	90.0	90.0	90.0	0.425
PN14	3.175	985.4	14.550	9.587	7.246	90.0	102.87	90.0	0.668
PN39	2.898	1072.8	12.730	8.177	10.643	90.0	104.45	90.0	0.583
CP13	1.978	1766.7	23.171	8.761	8.703	90.0	90.0	90.0	0.761
CP19	5.812	2732.4	11.117	8.769	28.029	90.0	90.0	90.0	0.831

[a]lengths are given in Å and angles are in degrees. RMS deviations are in Å. [b]The gradient norm is given in kcal/mol Å.

VSWITCH nonbond cutoff options are used in non-bonding energy evaluation. ABNR (Adopted Basis Newton-Raphson) minimization is performed with the crystal coordinates as the initial structure until the criteria for energy difference and gradient are satisfied. Both the tolerance values are set to 0.0. The crystal lattice parameters are also optimized by using the ABNR LATTICE option. The lattice constants *a*, *b* and *c* are optimized for orthorhombic crystals and *a*, *b*, *c* and β are optimized for monoclinic crystals.

Results and Discussion

As many research groups in antibiotics development have investigated the structure-activity relationship of penam and cephem derivative compounds, there are abundant crystal data of penams and cephems available in CSD. We have picked six crystals out of those available; four penam derivative and two cephem derivative crystals. In order to simulate crystal environments, we need the coordinates of all molecules in the unit cell present in the reported data set. The unit cell molecules are 6-(D-(-)-α-Aminophenyl-acetoamido)-penicillanic acid (AMPC),[13] p-Bromobenzyl-penicillin 1'-diethylcarbonate ester (PN09),[14] (2,6-Dimethoxyphenyl)-penicillin methyl ester (PN14),[15] Penicillin-G-acetoxymethylester (PN 39),[16] 4-Acetyl-3-methyl-7β-phenoxyacetamido-Δ^3-cephem (CP 13),[17] and 3-Amino-4-methoxy-cephalothin benzhydryl ester (CP19).[18] The molecular structures are depicted in Figure 1 and the crystal data are reproduced in Table 2.

The six crystals are non-trivial systems in routine molecular modeling research. The ampicilin molecules in the crystalline state (AMPC) exist as zwitterions and are modeled as specified in the CSD file. The PN09 crystal contains a covalently bonded bromine atom, which is one of the least studied atoms in molecular mechanics. In general, hydrogen positions are less accurately known than those of heavy atoms. The hydrogen H313 is not included in the PN09 crystallographic data and H102 is missing in the PN14 crystal coordinates. The "add H-atom" feature of QUANTA is used to place those missing hydrogens.

Crystal simulations are performed with repeating periodic boundaries, which are set up by the CRYSTAL facility working with the IMAGE module in CHARMM. Under the crystal cutoff distance of 15.0 Å, about 100 crystal images are considered in each model. The ABNR minimizer is employed to minimize crystal energy and forces (negative gradients). The minimization process exits the iteration loop when the gradient norm reaches the preset criterion, which warrants a

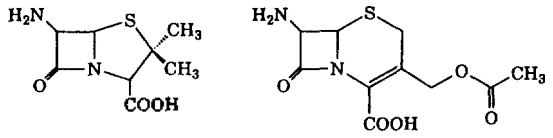

6-APA **7-ACA**

Figure 2. Molecular formulae for 6-APA (6-aminopenicillanic acid) and 7-ACA (7-aminocephalosporanic acid).

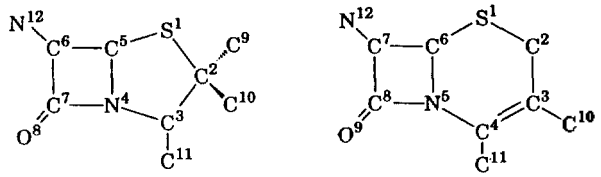

penam **cephem**

Figure 3. Penam and cephem core ring structures. Atoms are numbered to aid discussions. Note that the C10 position of cephem is the methyl carbon in CP13 and the amino nitrogen in CP19, respectively.

relaxed structure with the minimum (at least the local minimum) energy. The optimized crystal lattice constants are collected in Table 3. The RMS (root-mean-square) deviation is obtained by comparing the final optimized coordinates and the initial coordinates. No orientation of the final coordinate set is performed against the initial coordinates to reduce the RMS deviation value. The initial gradient norm values are also shown in Table 3, which reflect strain in the X-ray crystal coordinates. As shown in Table 3, all crystal lattice parameters are in excellent agreement with the corresponding crystallographic data; the lattice constants are preserved within 0.7 Å (the RMS deviation is 0.34 Å) with fixed contact angles during the entire optimization.

In this work, we examine the applicability of MMFF in evaluating molecular energies and forces of strained molecular moieties, the penam and cephem ring systems, in realistic and complex molecular environment. The optimized crystal geometries provide the basis for the force field evaluation. In order to examine the effectiveness of MMFF in representing complex molecular environments, we also perform geometry optimization of the isolated penam and cephem cores, 6-aminopenicillanic acid (6-APA) and 7-aminocephalosporanic acid (7-ACA). Their molecular formulae are given in Figure 2.

Table 4. Penam Core Bond Lengths[a]

Bond	AMPC		PN09		PN14		PN39		6-APA
	X-Ray	MMFF	X-Ray	MMFF	X-Ray	MMFF	X-Ray	MMFF	MMFF
S1 C2	1.854	1.857	1.859	1.850	1.841	1.855	1.857	1.852	1.855
C2 C3	1.556	1.538	1.564	1.549	1.554	1.546	1.567	1.550	1.547
C2 C9	1.482	1.518	1.527	1.537	1.539	1.527	1.523	1.536	1.538
C2 C10	1.511	1.524	1.518	1.531	1.528	1.534	1.529	1.533	1.533
C3 N4	1.466	1.476	1.468	1.461	1.449	1.461	1.450	1.456	1.457
C3 C11	1.566	1.545	1.495	1.531	1.522	1.526	1.511	1.529	1.524
N4 C5	1.466	1.475	1.476	1.471	1.486	1.475	1.457	1.466	1.474
N4 C7	1.382	1.367	1.367	1.369	1.389	1.378	1.378	1.369	1.369
C5 S1	1.812	1.822	1.815	1.835	1.805	1.835	1.815	1.838	1.840
C5 C6	1.528	1.536	1.561	1.548	1.551	1.544	1.546	1.549	1.553
C6 C7	1.528	1.544	1.541	1.548	1.536	1.542	1.542	1.550	1.548
C6 N12	1.430	1.489	1.440	1.489	1.433	1.476	1.420	1.484	1.472
C7 O8	1.181	1.212	1.201	1.210	1.196	1.208	1.202	1.210	1.209

[a]Atoms are defined in Figure 3. Bond lengths are given in Å.

Table 5. Cephem Core Bond Lengths[a]

Bond	CP13		CP19		7-ACA
	X-Ray	MMFF	X-Ray	MMFF	MMFF
S1 C2	1.813	1.825	1.836	1.800	1.821
C2 C3	1.507	1.523	1.511	1.524	1.518
C3 C4	1.337	1.353	1.355	1.353	1.354
C4 N5	1.414	1.355	1.424	1.372	1.362
C4 C11	1.488	1.502	1.423	1.504	1.487
N5 C6	1.445	1.446	1.472	1.472	1.451
N5 C8	1.396	1.350	1.349	1.371	1.353
C6 S1	1.795	1.806	1.811	1.804	1.816
C6 C7	1.566	1.549	1.565	1.551	1.562
C7 N12	1.429	1.489	1.454	1.474	1.473
C7 C8	1.543	1.556	1.520	1.552	1.562
C8 O9	1.210	1.211	1.219	1.212	1.209

[a]Atoms are defined in Figure 3. Bond lengths are given in Å.

2.

As shown in Figure 1, the MMFF energy minimization is applied to a variety of unit cell molecules. Instead of going over details of each molecular structure, we focus on the common molecular constructs in those penam and cephem molecules. The common molecular moieties are depicted and labeled in Figure 3.

The MMFF molecular geometry of optimized crystal structure is compared to that from crystallographic data. Core ring bond lengths are collected in Tables 4 and 5. Optimization with the MMFF parameter set reproduces bond lengths in excellent agreement to X-ray crystallographic data. The standard deviation of the bond lengths listed in the table is about 0.02 Å. We obtain better agreement for penams than for cephems. Most of penam ring bond lengths are reproduced within 0.015 Å. Lengths of the peripheral bonds, C2-C9, C2-C10, C3-C11, C6-N12 and C7=O8 are slightly more deviated from the corresponding crystal data. Similar results are obtained for cephem rings except for the bond between the sp^2 carbon to the sp^3 nitrogen, C4-N5, which deviates as much as 0.059 Å in CP13. An improvement in the MMFF parameter would be possible for the particular molecular construct.

Bond angles are compared in Tables 6 and 7. Bond angles in the penam core are reproduced with the average error of 1° and the standard deviation of 1.5°. Bond angles in cephems are correct to 2.5° in average with the standard deviation of 3°. Among the inner ring angles, the largest deviation from the crystallographic data is observed for N5-C6-S1; 4.9° in CP19. The β-lactam ring angles are especially well reproduced within 1° in most cases. The results indicate that MMFF is very effective in handling strained molecular angles and reflecting molecular environments.

We compare core ring dihedral angles in Tables 8 and 9. Overall comparison shows that MMFF optimization reproduces dihedral angles in penam crystal geometry within 5° in average and those in cephem crystal geometry within 9° in average. 10 degree deviation in dihedral angles is considered to be quantitative in molecular mechanical calculations. Small discrepancies in bond lengths and bond angles are amplified into the dihedral angle differences. The puckering of the five-membered ring and the six-membered ring is remarkably well reproduced. The four-membered β-lactam ring geometry is also in good agreement for both penam and cephem crystals. Although the β-lactam ring puckering is unique in each crystal and even that of 6-APA is quite different, it is quantitatively reproduced especially for penams. While the four membered ring is flat in the MMFF optimized 7-ACA structure, the significant ring puckering in cephem crystals is also well reproduced.

An improper dihedral angle reflects the displacement of the atom at the triatomic center from the plane containing three atoms bound to it. It is the quantitative expression of chirality. We examine four atoms of the β-lactam ring as the chiral center. The improper dihedral angles are listed in Tables 10 and 11 for penams and cephems, respectively. Most improper dihedral angles are in good agreement with

Table 6. Penam Core Bond Angles[a]

Angle	AMPC		PN09		PN14		PN39		6-APA
	X-Ray	MMFF	X-Ray	MMFF	X-Ray	MMFF	X-Ray	MMFF	MMFF
S1 C2 C3	103.1	102.5	103.9	106.0	103.2	103.5	105.0	107.0	106.8
S1 C2 C9	110.4	109.5	109.8	107.9	109.3	108.9	109.1	107.5	107.5
S1 C2 C10	109.5	108.2	108.6	107.7	110.7	108.0	108.3	107.8	108.0
S1 C5 C6	118.9	120.4	118.9	117.6	117.0	120.4	119.3	116.8	118.7
C2 C3 N4	106.0	105.6	105.6	107.0	107.4	107.6	106.0	107.3	107.4
C2 C3 C11	111.7	116.7	114.2	114.3	111.7	112.2	113.0	113.5	114.3
C3 N4 C5	117.9	117.9	115.8	117.2	115.9	117.8	117.2	117.6	117.5
C3 N4 C7	126.1	122.2	126.7	122.2	123.3	120.7	126.7	122.1	122.2
N4 C5 S1	103.8	103.3	105.5	105.3	103.1	102.7	105.8	105.6	105.0
N4 C5 C6	88.5	88.2	87.7	88.0	87.6	87.3	88.8	88.1	87.4
C5 S1 C2	90.4	90.6	95.2	95.0	89.6	90.7	94.9	94.6	94.9
C5 N4 C7	93.7	94.2	94.2	94.3	892.2	92.9	93.8	94.4	94.2
C5 C6 C7	85.7	85.1	84.4	84.5	84.4	84.2	84.2	84.3	84.4
C5 C6 N12	120.3	117.4	116.4	116.5	119.7	115.8	116.9	115.4	112.5
C6 C7 O8	138.1	136.9	134.6	136.8	137.3	138.5	137.4	136.9	136.6
C6 C7 N4	91.6	91.9	92.6	91.8	91.8	90.9	92.0	91.7	91.5
C7 C6 N12	115.8	117.2	116.7	115.9	119.6	121.9	116.6	115.0	115.3
O8 C7 N4	130.2	131.0	132.9	130.9	130.9	130.5	130.6	130.9	131.5

[a]Atoms are defined in Fig. 3. Angles are given in degrees.

Table 7. Cephem Core Bond Angles[a]

Angle	CP13		CP19		7-ACA
	X-Ray	MMFF	X-Ray	MMFF	MMFF
S1 C2 C3	117.7	115.3	110.1	113.7	113.1
S1 C6 C7	113.0	119.0	120.2	118.8	119.2
C2 C3 C4	125.7	124.0	119.5	119.5	122.9
C3 C4 N5	117.8	120.0	115.2	123.0	121.7
C3 C4 C11	125.1	121.9	124.4	120.8	120.8
C4 N5 C6	125.8	122.6	125.4	122.0	125.7
C4 N5 C8	132.6	139.2	131.2	122.8	133.9
N5 C6 S1	109.8	106.6	112.4	117.3	108.7
N5 C6 C7	87.5	86.5	86.8	86.9	86.9
C6 S1 C2	95.5	93.6	98.7	100.6	93.6
C6 N5 C8	95.1	97.8	94.4	93.6	97.6
C6 C7 C8	84.8	85.6	84.3	83.8	85.0
C6 C7 N12	121.2	117.3	122.2	121.7	113.2
C7 C8 O9	137.8	137.6	135.9	137.1	136.3
C7 C8 N5	90.2	89.7	93.2	90.5	90.4
C8 C7 N12	121.2	121.8	114.3	114.6	114.4
O9 C8 N5	131.9	132.6	130.9	132.4	133.1

[a]Atoms are defined in Figure 3. Angles are given in degrees.

the corresponding crystallographic data.

In medicinal chemistry research, it is believed that the pyramidality of the β-lactam nitrogen is closely related to the antibacterial activity.[11] The degree of pyramidality (approximately −25° in penams) is well preserved in penam crystals as well as in 6-APA (C3-N5-C7-N4). The MMFF parameter set is able to reproduce the improper angle within 2°. While the signs are correct, MMFF underestimates the improper angle (C4-C6-C8-N5) for CP13 and overestimates it for CP19. The 7-ACA value is in between the two, but is smaller than the crystal values. The C4-N5 connection might have caused the difficulty in MMFF calculations as pointed out in the discussion about bond lengths. The bond angles involving the C4-N5 bond are off by as much as 6.6° for C4-N5-C8 of CP13. We need to re-examine and possibly improve the MMFF parameters for the sp^2 carbon atom bound to a tricenter nitrogen atom.

The carbonyl carbon (C7 in penams and C8 in cephems) maintains the sp^2 hybridization and stay in the plane of the three atoms attached to it. Note that the small improper dihedral angle N5-C7-O9-C8 of CP13 flips the sign as compared to that of 7-ACA, which is also reproduced by MMFF crystal optimization.

The comparison shown in Tables 4 through 11 provides

Table 8. Penam Core Dihedral Angles[a]

Dihedral Angle	AMPC		PN09		PN14		PN39		6-APA
	X-Ray	MMFF	X-Ray	MMFF	X-Ray	MMFF	X-Ray	MMFF	MMFF
C5 S1 C2 C3	−40.3	−42.0	21.1	16.1	−40.9	−38.4	16.9	11.8	11.6
C5 S1 C2 C9	−159.1	−161.8	−97.4	−103.6	−158.6	−157.9	−100.4	−107.5	−107.6
C5 S1 C2 C10	78.5	79.3	141.9	140.2	79.3	83.1	138.1	135.8	135.6

S1 C2 C3 N4	34.0	38.3	−35.6	−29.0	31.0	30.3	−30.8	−24.9	−25.2
S1 C2 C3 C11	158.4	168.5	84.2	90.1	158.1	155.3	89.0	94.6	93.7
C2 C3 N4 C5	−9.7	−16.1	−144.6	−150.2	−2.9	−4.7	36.6	31.8	32.7
C2 C3 N4 C7	−128.3	−131.7	122.9	117.1	−114.7	−117.1	−81.9	−83.7	−82.4
C3 N4 C5 S1	−20.0	−14.9	−23.1	−20.9	−27.3	−23.5	−23.2	−22.2	−23.2
C3 N4 C5 C6	−139.5	−135.8	−142.5	−139.0	−144.5	−144.0	−143.4	−139.6	−142.2
C7 N4 C5 S1	114.6	115.2	111.4	108.8	101.7	103.7	111.8	107.6	106.6
C7 N4 C5 C6	−4.8	−5.7	−8.0	−9.4	−15.4	−16.8	−8.4	−9.7	−12.4
N4 C5 C6 C7	4.3	5.1	7.1	8.3	14.0	15.0	7.5	8.6	11.0
N4 C5 C6 N12	121.9	123.3	124.2	124.6	135.0	137.7	124.4	123.5	126.1
C5 C6 C7 N4	−4.6	−5.5	−7.7	−8.9	−15.0	−16.1	−7.9	−9.2	−11.8
C5 C6 C7 O8	173.6	171.2	172.3	162.7	163.0	160.9	169.7	162.3	161.2
O8 C7 N4 C3	−44.6	−44.4	−45.1	−37.0	−39.3	−35.6	−41.0	−36.0	−34.8
O8 C7 N4 C5	−173.6	−171.3	−171.8	−163.0	−162.6	−160.6	−169.4	−162.6	−161.2

[a] Atoms are defined in Figure 3. Angles are given in degrees.

Table 9. Cephem Core Dihedral Angles[a]

Dihedral Angle	CP13		CP19		7-ACA
	X-Ray	MMFF	X-Ray	MMFF	MMFF
C6 S1 C2 C3	−38.1	−41.6	52.9	41.1	−52.2
S1 C2 C3 C4	10.6	11.1	−55.6	−45.1	25.7
C2 C3 C4 N5	6.9	6.4	6.3	5.1	4.6
C2 C3 C4 C11	176.8	−174.0	−174.2	−171.8	−173.0
C3 C4 N5 C6	16.9	22.1	46.7	36.0	6.4
C3 C4 N5 C8	−127.3	−152.9	−91.4	−83.3	−150.3
C4 N5 C6 S1	−52.9	−62.1	−37.1	−29.7	−44.6
C4 N5 C6 C7	−166.5	178.6	−158.6	−150.7	−164.4
C8 N5 C6 S1	101.4	114.6	112.7	103.0	118.6
C8 N5 C6 C7	−12.1	−4.6	−8.8	−17.9	−1.2
N5 C6 C7 C8	10.9	4.0	7.8	15.9	1.0
N5 C6 C7 N12	134.5	127.7	123.0	131.0	115.5
C6 C7 C8 N5	−11.3	−4.3	−8.6	−17.0	−1.1
C6 C7 C8 O9	171.1	178.1	171.2	160.9	174.2
C7 C8 N5 C6	12.3	4.6	9.1	17.9	1.2
C7 C8 N5 C4	163.8	−179.6	156.0	150.1	162.2
O9 C8 N5 C6	−169.9	−177.6	−170.7	−160.2	−174.4
O9 C8 N5 C4	−18.4	−1.7	−23.8	−28.0	−13.3

[a] Atoms are defined in Figure 3. Angles are given in degrees.

Table 11. Cephem Core Improper Dihedral Angles[a]

Improper	CP13		CP19		7-ACA
Dihedral Angle	X-Ray	MMFF	X-Ray	MMFF	MMFF
C4 C6 C8 N5	−12.3	−1.6	−14.5	−22.7	−8.1
S1 C7 N5 C6	−37.9	−36.6	−33.0	−31.3	−35.5
C6 N12 C8 C7	−42.4	−44.7	−42.3	−42.5	−48.3
N5 C7 O9 C8	1.9	1.8	−0.2	−1.6	−3.6

[a] Atoms are defined in Figure 3. Angles are given in degrees.

Table 10. Penam Core Improper Dihedral Angles[a]

Improper	AMPC		PN09		PN14		PN39		6-APA
Dihedral Angle	X-Ray	MMFF	X-Ray	MMFF	X-Ray	MMFF	X-Ray	MMFF	MMFF
C3 C5 C7 N4	−23.6	−25.9	−24.3	−26.2	−26.5	−27.0	−23.5	−26.0	−26.0
S1 C6 N4 C5	−37.8	−37.2	−36.9	−37.9	−38.9	−37.6	−36.6	−38.3	−37.5
C5 N12 C7 C6	−42.5	−45.0	−46.7	−46.1	−44.0	−47.2	−46.4	−47.0	−49.3
N4 C6 O8 C7	−1.4	−2.5	0.0	−6.4	−1.5	−2.3	−1.8	−6.5	−5.3

[a] Atoms are defined in Figure 3. Angles are given in degrees.

strong indication of the viability of MMFF in modeling complex molecular systems in condensed phase. The ring core structure in crystals takes a variety of conformations different from the optimized structure of the isolated core molecule in vacuum. The crystalline structures are well reproduced with a single set of MMFF parameters, which can

be applied in modeling a vast range of new molecular interactions.

Ab initio techniques could be applied to a molecular system isolated in vacuum. To date, no *ab initio* calculation has been reported on the penam and cephem molecules. 238 basis functions over 464 primitive gaussians are required for *ab initio* calculations of 6-APA with the 6-31G* basis set, which is rather computationally demanding. A few *ab initio* calculations with 4-21G or 4-21G* basis set have been carried out for bicyclic β-lactams in conjunction with studying structure-activity relationships.[19] Those ring structures are the penam and cephem cores with the sulphur atom replaced by an oxygen atom or by a methylene group. There is a HF/6-31G** level calculation on 2-Azetidione (the four membered β-lactam ring with no substitution on methylene groups).[20] The MMFF optimized geometries in Tables 4-7 indicate that MMFF reproduces experimental bond lengths and bond angles in similar quality to *ab initio* calculations with the the 6-31G** basis set.

Semiempirical methods have been applied to penam and cephem geometry calculations.[21,22] The semiempirical calculations are intended to compute reaction paths and activation energetics. The MMFF results are superior to those MINDO/3, MNDO and AM1 calculations in reproducing crystal geometries. However, one should note that the crystalline environment is not considered in those semiempirical calculations.

Chung and Chodosh carried out the molecular mechanical calculations on selected sets of penams, cephems and monobactams.[23] Crystal bond lengths and bond angles were obtained in reasonable agreement to the experimental data, although the calculations did not include crystal environments. The MM2 and AMBER force fields used in the work might have taken care of the particular molecular constructs found in the penam and cephem molecules. The parametrization should have involved fair amounts of uncertainties and time consuming efforts. Here, MMFF is used as the universal force field in nature. While no fine tuning has been involved in this work, the crystalline state geometries are well reproduced.

Conclusion

One of the primary assumptions in molecular mechanics is that one can devise force fields for realistic systems (e.g., solutions and crystals of macromolecules) based on those obtained from accurate studies of small molecules. A large number of *ab initio* calculations on a comprehensive selection of small molecules have been the main basis for the MMFF development. The effective pair potentials are included for non-bonded interactions so that MMFF may handle molecular assemblies in condensed phase.

MMFF is a universal force field and no fine tuning has been made for the crystals of penams and cephems simulated in this work. We would expect that finely tuned molecular force fields against the particular system at hand would have generated more accurate conformations. However, the straightforward application of MMFF to crystalline states yields excellent results in reproducing the crystal geometries. Most crystalline molecular structures are reproduced within 0.02 Å for bond lengths and within 2.5° for bond angles. We have also obtained reasonably accurate molecular conformations in the crystal. In these regards, MMFF is quite promising for potential applications in macromolecular researches that involve new molecular constructs, e.g., researches on ligand receptor interactions, new drug design and polymer material developments.

MMFF has been implemented as a part of the CHARMM package (developmental). It is possible to use most of CHARMM molecular modeling facilities with evaluating energies and forces by MMFF. We have utilized the CHARMM minimizer as it is in the current version without further modification to use the MMFF parameter set. An energy minimization would not be the optimal choice for crystalline state simulations. Molecular dynamics simulation on the penam and cephem crystals are of further interests. The DYNAMICS facility of the CHARMM version used in this work does not support all crystal systems. The dynamics code is under developments to simulate dynamical behavior of those crystals optimized in this work.

Acknowledgment. The author thanks R. Czerminski for helpful discussions, E. Lim for preparing the crystal data from CSD, and W. Im for fixing the unit cell rotation problem in CHARMM. This work was supported by Cray Research, Inc. and by the Basic Science Research Institute Program, Ministry of Education of Korea (BSRI-94-3428).

References

1. Allinger, N. L. *J. Am. Chem. Soc.* **1977**, *89*, 8127.
2. Bukert, U.; Allinger, N. L. *Molecular Mechanics*; American Chemical Society: Washington, DC, 1982.
3. Allinger, N. L.; Yuh, Y. H., Lii, J.-H. *J. Am. Chem. Soc.* **1989**, *111*, 8551.
4. Weiner, S. J.; Kollman, P. A.; Nguyen, D. T.; Case, D. A.; Singh, U. C.; Ghio, C.; Alagona, G.; Profeta, S.; Weiner, P. *J. Am. Chem. Soc.* **1984**, *106*, 765.
5. Brooks, B. R.; Bruccoleri, R. E.; Olafson, B. D.; States, D. J.; Swaminathan, S.; Karplus, M. *J. Comput. Chem.* **1983**, *4*, 187.
6. Mayo, S. L.; Olafson, B. D.; Goddard, W. A. III *J. Phys. Chem.* **1990**, *94*, 8897.
7. Rappé, A. K.; Casewit, C. J.; Colwell, K. S.; Goddard, W. A III; Skiff, W. M. *J. Am. Chem. Soc.* **1992**, *114*, 10024.
8. Root, D. M.; Landis, C. R.; Cleveland, T. *J. Am. Chem. Soc.* **1993**, *115*, 4201.
9. Halgren, T. A. *J. Comp. Chem.* **1995**, *16*, in press.
10. Boyd, D. B. *Chemistry and Biology of β-Lactam Antibiotics* Vol. 1, Morin, R. B. & Gorman, M. Eds.; Academic Press: New York, 1982; p 500.
11. Boyd, D. B. *Int. J. Quantum Chem. Quantum Biol. Sympos.* **1977**, *4*, 161.
12. Halgren, T. A. *J. Am. Chem. Soc.* **1992**, *114*, 7827.
13. Boles, M. O.; Girven, R. J. *Acta Cryst. Sec.* B **1976**, *32*, 2279.
14. Csoregh, I.; Parm, T.-B. *Chem. Commun., Univ. Stockholm* 1976.
15. Blanpain, P.; Melebeck, M.; Durant, F. *Acta Cryst. Sec.* B **1977**, *33*, 580.
16. Labischinski, H.; Naumann, D.; Barnickel, G.; Dreissig, W.; Gruszecki, W.; Hofer, A.; Bradaczek, H. *Z. Naturforsch. Teil* B **1987**, *42*, 367.

17. Domiano, P.; Nardelli, M.; Balsamo, A.; Macchia, B.; Macchia, F.; Meinardi, G. *J. Chem. Soc. Perkin Trans.* 2 **1978**, 1082.
18. Spry, D. O.; Bhala, A. R.; Spitzer, W. A.; Jones, N. D.; Swartzendruber, J. K. *Tetrahedron Lett.* **1984**, *25*, 2531.
19. Fernández, B.; Carballeira, L.; Ríos, M. A. *Biopolymers* **1992**, *32*, 97.
20. Marstokk, K. M.; M llendal, H.; Samdal, S.; Uggerud, E. *Acta Chem. Scand.* **1989**, *43*, 351.
21. Frau, J.; Coll, M.; Donoso, J.; Munoz, F.; Garcia Blanco, F. *J. Molec. Struc. (Theochem)* **1991**, *231*, 109.
22. Frau, J.; Donoso, J.; Munoz, F.; García Blanco, F. *J. Molec. Struc. (Theochem)* **1991**, *251*, 205.
23. Chung, S. K.; Chodosh, D. F. *Bull. Korean Chem. Soc.* **1989**, *10*, 185.

Generalization of Keesom Transformation in Multipole-Multipole Interaction Potentials

Chun-Woo Lee

Department of Chemistry, Ajou University, 5 Wonchun Dong, Suwon 441-749, Korea
Received June 29, 1995

In order to ease the treatment of anisotropic potential when developing the variational RRKM theory, we applied Fano-Racah's recoupling theory to the multipole-multipole interaction, resulting in the great simplification of the anisotropic potentials. The treatment appears as a generalization of Keesom transformation in case of dipole-dipole interaction and provides us with great insights to the characteristics of tensorial interactions in the multipole-multipole interaction system.

Introduction

Recently, there have been considerable interests[1] in fast, neutral gas phase reactions with no potential barriers along the reaction coordinates. The interest derives from their important role in areas such as atmospheric, combustion and interstellar chemistry. Another source of interest is the progress in the experimental methods for detecting small concentrations of very reactive molecules such as free radicals.

The reaction rate constants for these reactions have often been found to decrease with increasing temperature.[1] Recent Rice Ramsperger Kassel Marcus (RRKM) variational calculations[2,3,4] have produced the same trends and several qualitative explanations are available now. We also succeeded in solving the variational RRKM equations analytically under some reasonable constraints and under the long-range potential of type $V(R, \Omega)=R^{-s}A(\Omega)$.[5] Here Ω stands for the angular variables and $A(\Omega)$ is the anisotropic part of the potential. For the fast neutral gas phase reactions with no potential barriers, it is believed that long range potentials play an important role.[6] Long-range potentials result from multipole-multipole interactions. They are tensor forces and have a complicated angular denpendence. Simple long-range-potentials that ignore the complicated angular dependence have thus enjoyed the frequent employ.

Long ago, Keesom[7] found an interesting transformation that greatly simplifies the angular part of the dipole-dipole interactions. Let us consider two dipoles A and B. Let (θ_1, ϕ_1) and (θ_2, ϕ_2) be their spherical polar coordinates. The z axis is directed toward each other. Then the angular dependence is given by $2\cos\theta_1\cos\theta_2-\sin\theta_1\sin\theta_2\cos(\phi_1-\phi_2)$. By considering the transformation, $2\cos\theta_1=g\cos\psi$, $\sin\theta_1=\theta_1=g\sin\psi$, Keesom showed that the angular dependenceis simplified as $g\cos\theta$. Thus Keesom transformation may be used to deal with the anisotropic nature of the dipole-dipole interaction.

On the other hand, Fano and Racah[8] discussed the tensorial nature of the dipole-dipole interaction in Appendix J of their book. The final formula surprisingly resembles Keesom transformation. We find that the final formula is actually equivalent to Keesom transformation. As Fano-Racah's approach can be easily generalized while Keesom transformation is not, we applied Fano-Racah's recoupling theory to the generalization of Keesom transformation. The result is surprisingly simple and takes the equivalent form of the simplest case of Keesom transformation. Our approach provides the insight to the nature of the anisotropic aspect of the multipole-multipole interactions which was not transparent in the past.

Keesom transformation and recoupling theory

Let us first summarize Fano-Racah's treatment of dipole-dipole interaction. The dipole-dipole interaction can be written as (see Appendix B. On the multipole expansion[9])

$$V=-(\vec{\mu}_1\cdot\nabla_1)(\vec{\mu}_2\cdot\nabla_2)\frac{1}{r}=(\vec{\mu}\cdot\nabla)(\vec{\mu}_2\cdot\nabla)\frac{1}{r}. \quad (1)$$

The last equality follows from $-\nabla_2=\nabla_1=\nabla$ that derives from $\vec{r}=\vec{r}_1-\vec{r}^2$. Now we can utilize the recoupling theory to recouple $(\vec{\mu}_1\cdot\nabla)$ and $(\vec{\mu}_2\cdot\nabla)$. We couple ∇ and ∇ together and $\vec{\mu}_1$ $\vec{\mu}_2$ together: